ORIGINAL ARTICLE

Stephen J. Bingham · Birgit Börger · Jörg Gutschank
Dieter Suter · Andrew J. Thomson

Probing the electronic structure of transition metal ion centres in proteins by coherent Raman-detected electron paramagnetic resonance spectroscopy

Abstract The simultaneous excitation of a paramagnetic sample with optical (laser) and microwave radiation can cause an amplitude or phase modulation of the transmitted light at the microwave frequency. The detection of this modulation indicates the presence of coupled optical and electron paramagnetic resonance (EPR) transitions in the sample. Here we report the first application of this technique to a biomolecule: the blue copper centre of *Pseudomonas aeruginosa* azurin. Using optical excitation at 686 nm, in the thiol to copper(II) charge transfer band, we measure a coherent Raman-detected EPR spectrum of a frozen aqueous solution. Its lineshape is characteristic of the magnetic circular dichroism along each principal *g*-value axis. This information allows electronic and structural models of transition metal ion centres in proteins to be tested.

Key words Electron paramagnetic resonance ·
Magnetic circular dichroism · Raman spectroscopy ·
Azurin · Copper

Introduction

Among the various spectroscopic techniques used for studying the electronic structures of transition metal ion centres in proteins, magnetic circular dichroism (MCD) [1] has proved particularly useful. It allows the optical spectra of two or more chemically distinct species in a single sample to be deconvoluted, pro-

vided their magnetic properties are sufficiently different. Conversely, if the optical bands of the two species are resolved, then their magnetic properties can be studied separately. In addition, the correlation of the optical and magnetic properties of a centre can allow the relative orientations of magnetic and optical anisotropies to be studied even in materials containing randomly oriented centres. The ability to perform such studies without the need to resort to single crystal absorption spectroscopy is particularly important in biological materials. Variable temperature MCD [1] spectroscopy distinguishes between centres through differences in the thermal distributions amongst magnetic ground states. However, the spin Hamiltonians of the centres may not be sufficiently different or anisotropic for such a separation to be feasible. In an attempt to overcome this disadvantage, one approach is to detect changes in the MCD brought about by microwave-induced changes in the populations of the magnetic states [2, 3]. However, a major drawback of this method is cross relaxation [4] between species that may remove both the chemical and orientational specificity of the experiment. In addition, lack of knowledge about the anisotropy of magnetic relaxation processes can make conclusions concerning the MCD anisotropy uncertain.

Coherent Raman-detected electron paramagnetic resonance (EPR) [5] has the potential to overcome these problems. As in a conventional EPR experiment, a signal proportional to the *transverse* magnetization precessing at the Larmor frequency is obtained. In contrast to the *longitudinal* magnetization that gives rise to the MCD, the transverse magnetization is not affected by cross relaxation unless microwave power saturation occurs. The technique presented here promises therefore a significant improvement in chemical and orientational specificity compared to traditional methods. In particular, knowledge of magnetic relaxation anisotropies is not required to allow conclusions to be drawn about MCD anisotropy. Coherent Raman-detected magnetic resonance spectroscopies

S.J. Bingham (✉) · B. Börger · J. Gutschank · D. Suter
Fachbereich Physik, Universität Dortmund
D-44221 Dortmund, Germany
e-mail: stephen.bingham@e3.physik.uni-dortmund.de
Fax: +49-231-7553516

A.J. Thomson
Centre for Metalloprotein Spectroscopy and Biology
School of Chemical Sciences, University of East Anglia
Norwich, NR4 7TJ, UK

have previously been used to study Zeeman splittings in alkali atom gases [6, 7], nuclear quadrupole resonance of lanthanide ions [7–9], spin waves in transition metal ion magnets [10, 11], and EPR of a colour centre [12], a semi-conductor [13], and chromium ions in ruby [5].

Principle of detection

The term "coherent Raman spectroscopy" was first used in the context of high-resolution laser spectroscopy of vibrational transitions, but the same theoretical formalism is now much more widely applied [8, 9]. Figure 1 illustrates its application to this experiment; three stationary states are required, connected by two optical transitions and an EPR transition. If the EPR transition $|1> \leftrightarrow |3>$ is excited with microwave radiation and the optical transition $|1> \leftrightarrow |2>$ with a laser, then light will be emitted by the transition $|2> \leftrightarrow |3>$ provided that it has a significant transition dipole. The frequency of the emitted Raman wave is equal to the sum or difference of the laser and microwave frequencies, depending on the energy of the states $|1>$, $|2>$, and $|3>$.

While the description of the experiment in terms of coherent Raman scattering has been used successfully, an alternative picture derived from MCD spectroscopy is sometimes more useful: the transverse magnetization induces a circular dichroism for light propagating through the sample in a direction perpendicular to the static magnetic field [6, 14]. For a given circular polarization, the Larmor precession modulates the sample absorbance at the microwave frequency. This model is quantitatively valid as long as the optical linewidth is large compared to the microwave frequency and provided that optical hole-burning effects are absent. In this case we may continue to use the concept of an optical transition probability on a timescale short compared to the microwave period [14]. This in turn allows us to describe the experiment using the well-established theories of conventional EPR [15] and magneto-optics [16]. We shall emphasize this picture in the current paper, while retaining the name "coherent Raman-detected EPR" to maintain consistency with the previous physics literature. The broad vibronic optical bands shown by metalloproteins make optical

Fig. 1 A three-level coherent Raman process
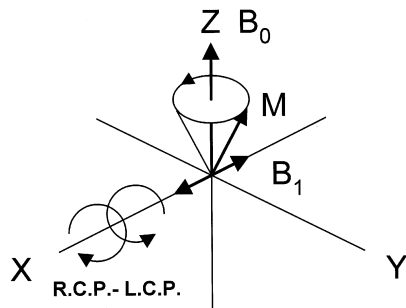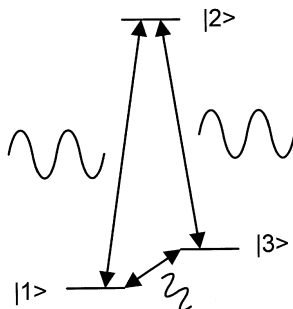
Fig. 2 Experimental geometry showing the applied magnetic field B_0, microwave field B_1, precessing magnetization M, and circularly polarized optical beam

hole burning unlikely and are always much wider than microwave frequencies.

The optimal experimental geometry is shown in Fig. 2. In an EPR experiment [15] the magnetization M precesses about the applied magnetic field B_0 in response to stimulation by an orthogonal microwave field B_1. An optical beam propagating along an axis X perpendicular to B_0 will experience a sinusoidally oscillating circular dichroism or circular birefringence, the size of which may be calculated using the theories of MCD [16] and Faraday rotation, respectively. Hence a circularly polarized beam will be amplitude modulated at the microwave frequency by the oscillating MCD. Changing the circular polarization from left to right will change the sign of the modulation. In the "coherent Raman picture", this modulation arises from the interference between the transmitted optical excitation and the Raman waves on the photodetector [6–9].

To apply this experiment to metalloproteins, it is essential to use a microwave frequency greater than 1 GHz in order to resolve g-value anisotropies. For this purpose, we have built an optical heterodyne instrument that operates at 14 GHz. A fast photodiode detects the microwave frequency modulation of the optical beam. Tests on our instrument have shown that it can detect six visible Raman photons in the presence of 10^{16} transmitted optical excitation photons (1 mW) with a 1 s data collection time [17]. In practice, this translates into a noise floor of a few parts in 10^{-8} modulation of the sample absorbance (see Fig. 4). This performance is considerably better than that of the Fabry-Perot interferometer-based instruments previously used to measure microwave frequency coherent Raman-detected magnetic resonance experiments [10, 11, 13]. It also compares favourably with polarimeters of the type typically used in MCD spectroscopy [1] that have a noise floor of $\cong 10^{-5}$ in absorbance. It is the development of this new instrument that makes study of biological transition metal ion centres feasible for the first time.

Materials and methods

A buffered aqueous solution of the protein *Pseudomonas aer-uginosa* azurin was mixed with a glassing agent (glycerol, 1:1 v/v) so that the sample remained optically transparent when frozen. A concentration of 3.2 mM was estimated from the optical absorbance. As shown in Fig. 3, the sample S is held in the centre of a TE_{102} rectangular microwave cavity in a cuvette made from two fused silica discs and a PTFE spacer. A circularly polarized laser beam passes parallel to the microwave frequency magnetic field through holes in the cavity. A semiconductor laser was used with an optical wavelength of 686 nm, close to the main thiol-copper(II) charge transfer band. The incident and transmitted powers, adjusted for reflections from cryostat windows, were approximately 6.3 mW and 2.1 mW, respectively. The optical path length was 0.5 mm. The intensity modulation of the transmitted light beam was measured using a high-speed photodiode and low-noise microwave receiver. A single microwave oscillator is used to excite the sample and drive the microwave receiver. This allows the phase relationship between the microwave excitation and the optical modulation to be examined and hence spectra analogous to conventional EPR absorption and dispersion spectra to be obtained. Use of a quadrature mixer enables the spectra of both phases, I and Q, to be measured simultaneously. In addition, the polarization of the light is modulated between left and right circularly polarized at 50 kHz using a photoelastic modulator (PEM), and the signals synchronously detected with lock-in amplifiers. The data are presented in terms of the microwave modulation of the absorbance ΔA of circularly polarized light according to:

$$P = P_0 \times 10^{-A}, \; A = A_0 + \frac{\Delta A}{2}\sin(\omega_1 t) \tag{1}$$

where P is the transmitted optical power, P_0 is the incident power, $\omega_1/2\pi$ is the microwave frequency, and A_0 is the average absorbance. A magnetic field perpendicular to the optical beam was provided by a superconducting spectroscopic magnet system (10^{-4} homogeneity over 1 cm diameter sphere; Oxford Instruments, Oxford, UK).
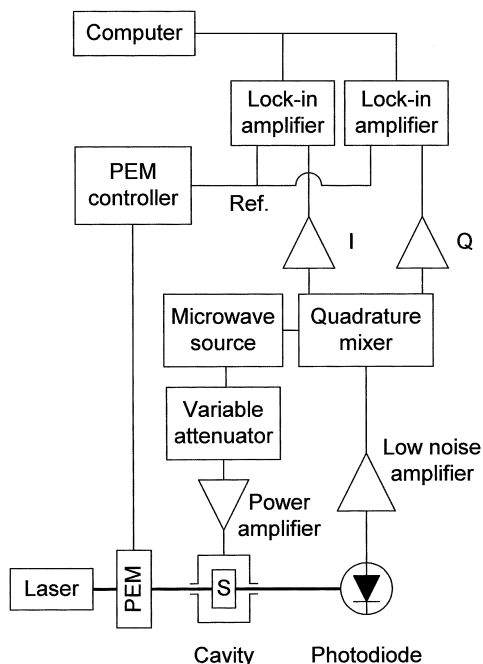
Fig. 3 Schematic diagram of the instrument

Results

Figure 4 shows coherent Raman-detected EPR spectra of *Ps. aeruginosa* azurin. At 1.8 K (Fig. 4a) the dispersion signal dominates the spectrum because the absorption signal is strongly microwave power saturated under these conditions. When the temperature is increased the rapid increase in spin-lattice relaxation rate [15, 18] allows the sample to absorb more microwave power and hence an absorption signal appears (Fig. 4b). For an inhomogeneously broadened line, the absorption signal is expected to be more easily microwave power saturated than the dispersion signal [19]. Nevertheless, some microwave power saturation of the dispersion signal at 1.8 K is indicated by the broadening of the line shape and the fact that the signal is significantly smaller than would be expected from a simple Curie law (signal $\propto$ 1/temperature) dependence. Microwave power dependence experiments gave no evidence for saturation of the dispersion signal at 1.7 or 48 K with microwave fields
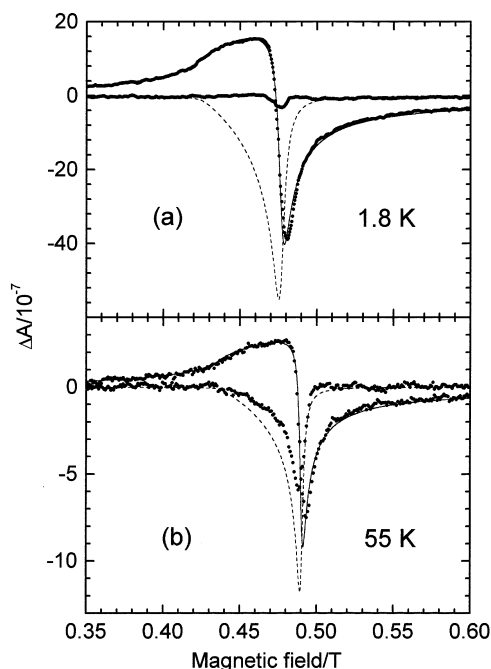

Fig. 4 a,b Coherent Raman-detected EPR spectra (*points*) of oxidized *Pseudomonas aeruginosa* azurin measured at 686 nm. The sample temperature, measured at the microwave cavity, was 1.8 K and 55 K for spectra **a** and **b**, respectively. The linearly polarized microwave field had a frequency of 13.67 GHz and an amplitude of approximately 50 µT for spectrum **a** and a frequency of 14.04 GHz and amplitude of 75 µT for spectrum **b**. The relative sizes of the absorption (*dashed lines*) and dispersion (*solid lines*) phase simulated lineshapes are those expected in the absence of microwave power saturation. Since no magnetic field modulation is used in the instrument, the spectra are presented as the absolute signals rather than the first derivatives commonly used in conventional EPR spectroscopy. The spectra have opposite sign to the conventional EPR signal because the MCD is negative at the monitored wavelength

between $\cong 10$ and $100~\mu T$, whereas the absorption signal could be easily saturated by increasing the microwave power at 48 K. This further indicates that the saturation of the dispersion is a weak effect.

Optical power-dependent studies show no evidence that spurious optical effects are important in determining lineshapes. Further, at 1.8 K the dispersion signal is linear with optical power between 1 and 8 mW incident power. We have verified that no intensity modulation of linearly polarized light is observed. The requirement of circularly polarized light is consistent with the signal resulting from the modulation of the MCD. Estimates of the signal size calculated from conventional EPR and MCD data also agree with our measurements.

Interpretation and simulation

The observed coherent Raman-detected EPR lineshapes (Fig. 4) differ considerably from those of the conventional EPR experiment (Fig. 5c). This is due to the contribution of the optical anisotropy to the coherent Raman-detected experiment. Only the part of the MCD arising from population differences between the magnetic states [16] will contribute to the coherent Raman-detected EPR signal. Although the MCD of an individual molecule can show a very complex orientational dependence, only certain terms contribute when an orientational average is carried out. For a
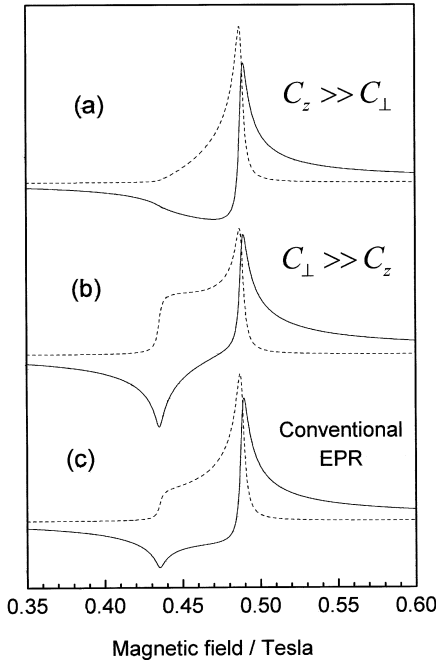
Fig. 5 a–c Simulated coherent Raman-detected EPR lineshapes of azurin for two limiting cases of MCD anisotropy. The lineshapes predicted for **a** $C_z > > C_\perp$ and **b** $C_\perp > > C_z$ are shown. The *dashed lines* are the absorption phase and *solid lines* are the dispersion phase lineshapes. The conventional EPR lineshapes simulated using the same model are shown in **c**

molecule with a fictitious spin 1/2 ground level, the relevant parts of the MCD observed along the laboratory X axis are:

$$\Delta\epsilon_X = 4Kf(v, v_{eg}, \Delta_{eg})\left[A_{Xx}C_x\tilde{S}_x + A_{Xy}C_y\tilde{S}_y + A_{Xz}C_z\tilde{S}_z\right];$$

(2)

where $\Delta\varepsilon_X$ is the difference in molecular extinction coefficients for left and right circularly polarized light $(\varepsilon_L - \varepsilon_R)$, K is a collection of fundamental constants $(N_A\alpha^2\pi\log(e)/1000\,\varepsilon_0 cn)$, v is the optical frequency, $f(v, v_{eg}, \Delta_{eg})$ is a normalized optical lineshape function $(\int \frac{f(v, v_{eg}, \Delta_{eg})}{v}dv = 1)$, A_{Xx}, A_{Xy}, A_{Xz} are the directional cosines between the laboratory X axis and each g-value axis and $\tilde{S}_{x,y,z}$ are the components of the molecular fictitious spin along each g-value axis. The parameters $C_{x,y,z}$ take the following form when expressed in terms of optical transition dipoles:

$$C_x = Im\left\{\sum_e \langle g(x)|m_y|e\rangle\langle e|m_z|g(x)\rangle\right\};$$

$$C_y = Im\left\{\sum_e \langle g(y)|m_z|e\rangle\langle e|m_x|g(y)\rangle\right\};$$

(3)

$$C_z = Im\left\{\sum_e \langle g(z)|m_x|e\rangle\langle e|m_y|g(z)\rangle\right\};$$

where $|g(x)\rangle$, $|g(y)\rangle$, $|g(z)\rangle$, are the ground level basis functions with $\tilde{S}_x = \frac{1}{2}, \tilde{S}_y = \frac{1}{2}, \tilde{S}_z = \frac{1}{2}$, respectively, $|e\rangle$, are the excited level states, and $m_{x,y,z}$ are electric dipole operators along the g-value axes. The parameters $C_{x,y,z}$ are closely related to the "C-terms" that are widely used to describe the paramagnetic part of the MCD signal [16]. The MCD C-term observed along the g-value x, y, and z axes are proportional to C_xg_x, C_yg_y, and C_zg_z, respectively. The g-value enters the C-term through its influence on the fictitious spin thermal polarization. In the present treatment the fictitious spin polarization is included within $\tilde{S}_{x,y,z}$.

Calculation of the coherent Raman-detected EPR signal in terms of the parameters $C_{x,y,z}$ mainly involves solving the equation of motion of the fictitious spin to obtain the parts of $\tilde{S}_{x,y,z}$ that oscillate at the microwave frequency, $\omega_1/2\pi$. For a set of molecules with an approximately axial g-value system, $g_\perp = g_x \cong g_y$, we find that the terms that oscillate in phase with M_X, the component of the magnetization responsible for the conventional EPR absorption and dispersion signals, take the form:

$$\Delta A_X(\omega_1) \propto T(\theta)f(\theta)\left[C_z\left(\frac{g_\perp^2 g_z}{g^2}\right)\sin^2\theta + C_\perp\left(\left(\frac{g_\perp g_z^2}{g^2}\right)\cos^2\theta + g_\perp\right)\right];$$

(4)

where θ is the angle between the g-value z axis and the magnetic field B_0, and g is the g-value:

$$g^2 = g_z^2 \cos^2 \theta + g_\perp^2 \sin^2 \theta \qquad (5)$$

$T(\theta)$ is a Boltzmann factor:

$$T(\theta) = \tanh\left(\frac{g\beta B_0}{2kT}\right); \qquad (6)$$

$C_\perp$ is the average MCD C-term in the g-value xy plane, $(C_x + C_y)/2$, and $f(\theta)$ is a lineshape factor. Although components of the fictitious spin oscillating in phase quadrature with M_X also exist, the resulting signal disappears when an orientational average is performed.

Azurin spectral lineshapes simulated using the above model are shown in Fig. 5. Simple Lorentzian lineshape functions $f(\theta)$ were used:

$$f(absorption) = \frac{\delta^2}{\delta^2 + (\omega_1 - \omega_0)^2},$$
$$f(dispersion) = \frac{\delta(\omega_1 - \omega_0)}{\delta^2 + (\omega_1 - \omega_0)^2} \qquad (7)$$

where δ is a linewidth parameter and $\omega_0/2\pi = g\beta B_0/h$ is the Larmor frequency. Excellent fits to the experimental lineshapes at both 1.8 and 55 K are obtained when $C_z >> C_\perp$ (Fig. 4). Only the linewidth parameter δ needs to be varied between the two temperatures (90 MHz at 1.8 K, 50 MHz at 55 K). It is important to note that data measured under very different experimental conditions lead to the same conclusion concerning MCD anisotropy. This makes it extremely unlikely that spurious effects such as magnetic relaxation or optical pumping anisotropy are significant in determining the lineshapes. Our observation that $C_z >> C_\perp$ is qualitatively consistent with the MCD-detected EPR lineshapes observed by Barrett et al. [2] provided that the magnetic relaxation is not too anisotropic in that experiment.

MCD anisotropy is a powerful probe of electronic structure through its dependence on the relative orientation of magnetic and optical anisotropies. The observation that $C_z \neq 0$ requires that the optical transition has an elliptical transition dipole in the xy plane of the g-value axis system. The absence of a C-term in the g-value xy plane either requires the absence of a dipole along the g-value z axis, or places certain constraints on the phase of that dipole relative to those in the xy plane. More specific conclusions can be made within the context of a particular model of electronic structure. In the model proposed by Gewirth and Solomon [20–22] for the blue copper centre of plastocyanin, the unpaired electron resides principally in the $d_{x^2-y^2}$ orbital but with significant delocalization onto the cysteine ligand. In the present context it is convenient to redefine the axis system so that x lies along the Cu-cysteine bond (Fig. 6). Single crystal EPR experiments [23] have shown that the g-value z axis lies approximately orthogonal to this bond. The rotation

of the axis system causes the $d_{x^2-y^2}$ and d_{xy} designations to be interchanged and the d_{xz+yz}, d_{xz-yz} orbitals considered by Gewirth and Solomon [20] to become d_{xz}, d_{yz}. In our axis system, a ligand field calculation predicts ground level wavefunctions of the form:

$$|g(z)\rangle \cong \left(|d_{xy}\rangle + \frac{\lambda i}{\Delta_{x^2-y^2}}|d_{x^2-y^2}\rangle\right)|+\rangle$$
$$- \left(\frac{\lambda}{2\Delta_{yz}}|d_{yz}\rangle + \frac{\lambda i}{2\Delta_{xz}}|d_{xz}\rangle\right)|-\rangle,$$
$$|\bar{g}(z)\rangle \cong \left(|d_{xy}\rangle - \frac{\lambda i}{\Delta_{x^2-y^2}}|d_{x^2-y^2}\rangle\right)|-\rangle \qquad (8)$$
$$+ \left(\frac{\lambda}{2\Delta_{yz}}|d_{yz}\rangle - \frac{\lambda i}{2\Delta_{xz}}|d_{xz}\rangle\right)|+\rangle$$

where $|\bar{g}(z)\rangle$, is the Kramers' conjugate of $|g(z)\rangle$, $|+\rangle$, $|-\rangle$, are the true spin functions quantized along the g-value z axis, $|d_{xy}\rangle$, $|d_{x^2-y^2}\rangle$, $|d_{xz}\rangle$, $|d_{yz}\rangle$, are the real d-orbitals, λ is the spin-orbit coupling constant and $\Delta_{x^2-y^2}$, Δ_{xz}, Δ_{yz} are the energies of the excited d-orbital levels. The splitting of the $|+1\rangle$, $|-1\rangle$, d-orbital set into $|d_{xz}\rangle$, $|d_{yz}\rangle$, implies that the g-value x and y axes lie parallel and perpendicular to the Cu-cysteine bond. The analogous band in plastocyanin to the one we are studying here has been assigned by Gewirth and Solomon as a charge transfer transition from an orbital with mainly cysteine p_y character:

$$|e\rangle \cong |p_y\rangle|+\rangle; \qquad (9)$$
$$|\bar{e}\rangle \cong |p_y\rangle|-\rangle;$$

Such an orbital will overlap well with the d_{xy} orbital (Fig. 6a) and hence give rise to an intense transition. Further, spin-orbit coupling will mix only small amounts of the other d orbitals into the ground level. This means that the transitions $|g\rangle \rightarrow |e\rangle$, $|\bar{g}\rangle \rightarrow |\bar{e}\rangle$, will make the major contribution to the MCD. The transition dipole $\langle p_y|r|d_{xy}\rangle$, is polarized along the g-value x axis (Fig. 6a), while the transition dipole $\langle p_y|r|d_{x^2-y^2}\rangle$,

Fig. 6 a,b. Schematic illustration of the transition dipoles between the cysteine sulfur p_y orbital and two copper d orbitals. The axis system used to discuss the polarization of the optical transitions is shown
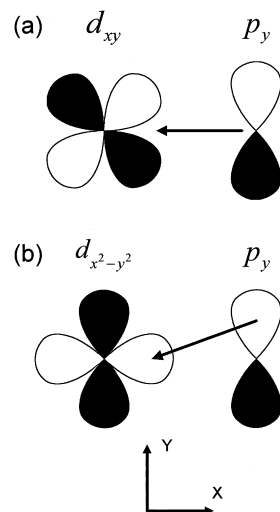
is linearly polarized along another axis in the *xy* plane (Fig. 6b). The physical significance of the occurrence of $|d_{x^2-y^2}\rangle$, in $|g\rangle$, as a pure imaginary admixture is that the associated dipole $\langle p_y|r|d_{x^2-y^2}\rangle$, oscillates in phase quadrature to the main dipole $\langle p_y|r|d_{xy}\rangle$. The result is that the transitions $|g\rangle \rightarrow |e\rangle$, and $|\bar{g}\rangle \rightarrow |\bar{e}\rangle$, have opposite elliptical polarizations in the *xy* plane and will therefore generate an MCD *C*-term along the *g*-value *z* axis. Since the transition dipoles $\langle p_y|r|d_{xz}\rangle$, and $\langle p_y|r|d_{yz}\rangle$, are expected to be strongly *x* polarized, with little or no *z* polarization, the MCD *C*-terms along the *g*-value *x* and *y* axes are expected to be very weak. The MCD anisotropy observed by coherent Raman-detected EPR is therefore found to be consistent with the assignment of the analogous transition made previously. The model considered here is also consistent with the polarized single crystal optical and EPR data of Penfield et al. [23]. More detailed calculations will be pursued once data from additional bands have been processed.

Conclusion

The experiments reported here illustrate the feasibility of using coherent Raman-detected EPR spectroscopy to study the electronic structures of biological transition metal ion centres. MCD anisotropies, relative to the *g*-value axis system, will be obtainable with far greater accuracy than from conventional MCD spectroscopy. Further, coherent Raman-detected EPR should be able to provide this information in centres, such as molybdenum(V) and iron-sulfur clusters, whose *g*-value anisotropies are too small to be distinguished with MCD saturation spectroscopy. In samples containing several types of transition metal ion centre, the high resolution of EPR spectroscopy should allow the optical spectra of species with very similar magnetic properties to be studied separately. In addition, since many important enzymes contain several transition metal centres, the ability to study each centre separately may allow, for example, perturbations due to interactions between centres to be identified. These experiments will provide a more complete picture of transition metal centres in metalloproteins.

References

1. Thomson AJ, Cheesman MR, George SJ (1993) Methods Enzymol 226:199–231
2. Barrett CP, Peterson J, Greenwood C, Thomson AJ (1986) J Am Chem Soc 108:3170–3177
3. Thomson AJ, Greenwood C, Peterson J, Barrett CP (1986) J Inorg Biochem 28:195–205
4. Bloembergen N, Shapiro S, Pershan PS, Artman JO (1959) Phys Rev 114:445–459
5. Bingham SJ, Suter D, Schweiger A, Thomson AJ (1997) Chem Phys Lett 266:543–547
6. Dehmelt HG (1957) Phys Rev 105:1924–1925
7. Suter D (1997) The physics of laser atom interactions. Cambridge University Press, Cambridge
8. Wong NC, Kintzer ES, Mlynek J, DeVoe RG, Brewer RG (1983) Phys Rev B 28:4993–5010
9. Blasberg T, Suter D (1995) Phys Rev B 51:12439–12450
10. Sandercock JR (1982) Top Appl Phys 51:173–206
11. Borovik-Romanov AS, Kreines NM (1982) Phys Rep 81:351–408
12. Holliday K, He XF, Fisk PTH, Manson NB (1990) Opt Lett 15:983–985
13. Romestain R, Geschwind S, Devlin GE, Wolff PA (1974) Phys Rev Lett 33:10–14
14. Bloembergen N, Pershan PS, Wilcox LR (1960) Phys Rev 120:2014–2023
15. Abragam A, Bleaney B (1970) Electron paramagnetic resonance of transition ions. Oxford University Press, Oxford
16. Stephens PJ (1976) Adv Chem Phys 35:197–264
17. Bingham SJ, Börger B, Suter D, Thomson AJ (1998) Rev Sci Instrum 69:3403–3409
18. Drews AR, Thayer BD, Stapleton HJ, Wagner GC, Giuliarelli G, Cannistraro S (1990) Biophys J 57:157–162
19. Portis AM (1953) Phys Rev 91:1071–1078
20. Gewirth AA, Solomon EI (1988) J Am Chem Soc 110:3811–3819
21. Solomon EI, Baldwin MJ, Lowery MD (1992) Chem Rev 92:521–542
22. Holm RH, Kennepohl P, Solomon EI (1996) Chem Rev 96:2239–2314
23. Penfield KW, Gay RR, Himmelwright RS, Eickman NC, Norris VA, Freeman HC, Solomon EI (1981) J Am Chem Soc 103:4382–4388